CHAPTER IV

RESULTS AND DISCUSSION

1. Determination of physicochemical properties of AZT

1.1 Determination of dissociation constant (pK_a) of AZT by spectrophotometric method

The UV-spectra of AZT at fourteen different pH values from 5.0 – 11.5 are shown in Figure 7. AZT showed the maximum absorption wavelength at 267 nm. The plot of AZT's absorbance against pH value was displayed in Figure 8. The absorbance of the unprotonated species (A_o) and protonated species (A_α) can be determined by drawing a straight line from a plateau of absorbance parallel to x-axis, to intercept the y-axis. The absorbance values for A_o and A_α were found to be 0.645 and 0.800, respectively. The pK_a of AZT was postulated to be the pH value at the midpoint of absorbance profile to be approximately 9.8 – 10.0. From eqn.8 and 9, the more exact pK_a value of AZT can be determined by comparing with the similarity factor value. It was found that the pK_a of AZT would be 9.9 at the highest similarity factor (f_2) of 99.9982 as comparing to pK_a at 9.8 and 10.0 as tabulated in Table 12.

From Figure 7 and Table 11, the maximum absorbance of AZT at 267 nm was decreased when pH value increased. It was observed that the pH values of those AZT solutions did not change during the experiment, which indicated sufficient buffer capacity of the systems.

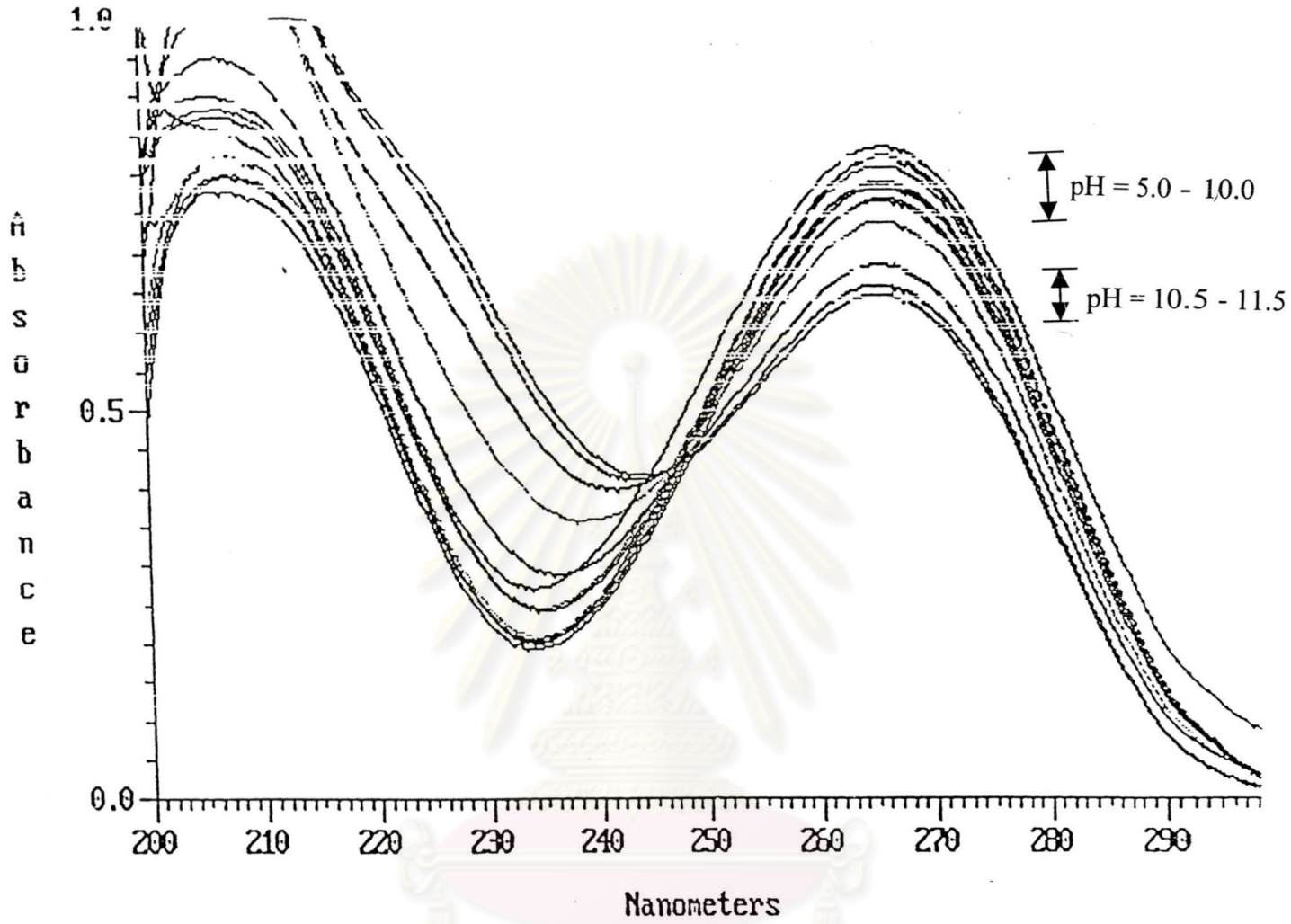

Figure 7 UV spectra of AZT $1x10^{-7}$ M in buffer at pH values between 5.0 to 11.5. (Each spectrum represents; one pH value.)

Table 11 UV absorbance of AZT in buffer solution pH 5.0-11.5 at 267 nm

pH of buffer solution	pH of AZT solution ($1x10^{-7}$ M, μ 0.1 M)	Absorbance of AZT (SD) (n=3)
5.0	5.02	0.785 (0.02)
5.5	5.50	0.792 (0.02)
6.0	6.00	0.822 (0.00)
6.5	6.00	0.778 (0.02)
7.0	7.03	0.813 (0.00)
7.5	7.53	0.785 (0.04)
8.0	7.98	0.817 (0.00)
8.5	8.60	0.799 (0.00)
9.0	8.95	0.788 (0.01)
9.5	9.48	0.760 (0.01)
10.0	10.05	0.716 (0.00)
10.5	10.43	0.664 (0.01)
11.0	10.95	0.646 (0.00)
11.5	11.40	0.644 (0.00)

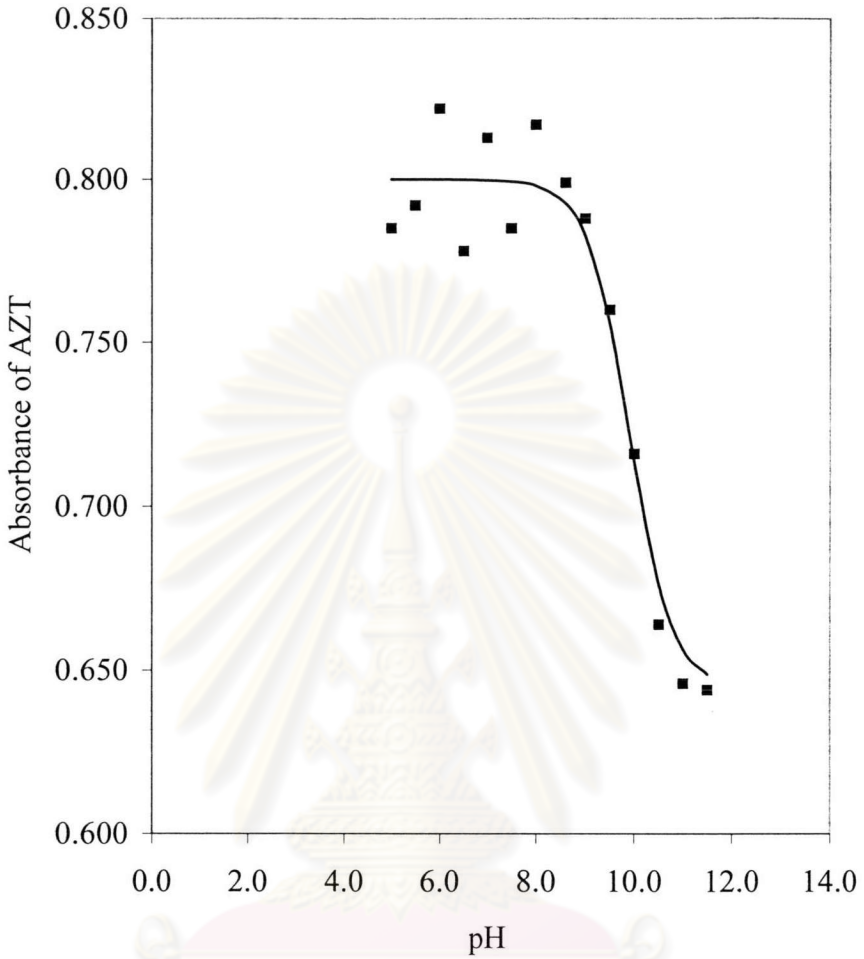

Figure 8 AZT absorbance as a function of pH value for pK_a determination of AZT at 267 nm. ;

_____ calculated absorbance; ■ experimental absorbance

Table 12 Determination of similarity factor

pH	Experimented absorbance (A′)	Calculated absorbance (A)		
		A (pk_a=9.8)	A (pk_a=9.9)	A (pk_a=10.0)
5.0	0.785	0.800	0.800	0.800
5.5	0.792	0.800	0.800	0.800
6.0	0.822	0.800	0.800	0.800
6.5	0.778	0.800	0.800	0.800
7.0	0.813	0.800	0.800	0.800
7.5	0.785	0.799	0.799	0.800
8.0	0.817	0.798	0.798	0.798
8.6	0.799	0.791	0.793	0.794
9.0	0.788	0.779	0.783	0.786
9.5	0.760	0.748	0.756	0.763
10.0	0.716	0.705	0.714	0.723
10.5	0.664	0.671	0.676	0.682
11.0	0.646	0.654	0.656	0.659
11.5	0.644	0.648	0.649	0.650
Similarity factor (f_2)		99.9980	99.9982	99.9979

Since the pK_a of AZT was determined to be 9.9 AZT would whether be a very strong basic or very weak acidic compound. The solubility of AZT in 0.1 N HCl and 0.1 N NaOH was then determined. The solubility value of AZT in 0.1 N NaOH was equal to 125.86 mg/ml that was almost four times the solubility of AZT in 0.1 N HCl (27.94) mg/ml.

Therefore, it was confirmed that AZT would be very weak acedic compound such that in strong alkali, AZT was dissociated and more solubilized than in acidic solution.

1.2 AZT Partition coefficient (K_{app}) determination

The apparent partition coefficients (K_{app}) of AZT between several non-aqueous phases and 0.01M phosphate buffer pH 7.4 are shown in Table 13. It was observed that, the K_{app} and log K_{app} value of AZT between several non-aqueous phases and 0.01M phosphate buffer pH 7.4 increased as the dielectric constant of the solvent increase. This indicates the more partitioning of AZT into the non-aqueous phase as its polarity increases. This performance confirms the hydrophilicity of AZT. In addition, log K_{app} value of AZT decreased as the number of carbon atom of alcoholic solvent was increased from 6 to 10 as presented in Figure 9.

Among these hydrophobic solvents used, it is known that the property of octanol is quite similar to the skin. In addition, water is solubilized to some extent in the octanol phase thus make it more useful to represent biological membrane.

From Table 13, AZT shows the log K value between octanol and phosphate buffer pH 7.4 to be 0.02 as similar to that reported by Seki's (Seki, Kawaguchi, and Juni, 1990). Since, the log K value between octanol-phosphate buffer at pH 7.4 can be implied the partitioning of compound into biological membrane, the log K value between zero and one can indicate the diffusion of compound into the stratum corneum and partitioning into the underlying tissue (Chein, 1992). According to these informations, AZT with log K value of 0.02 would possibly be able to transport through diffused into the stratum corneum and partitioning into the underlining tissue.

Table 13 Apparent partition coefficients, K_{app}, of AZT[a]

Non-aqueous phase	Dielectric constant (ε)[c]	AZT (n=3)	
		K_{app} (SD)	Log K_{app} (SD)
Hexane	1.89 (25°C)	0 (0.03)	-[b]
Carbon Tetrachloride	2.24 (20°C)	0 (0.1)	-[b]
Chloroform	4.81 (20°C)	0.23 (0.10)	-0.64 (0.02)
n-decanol	8.10 (20°C)	0.64 (0.08)	-0.20 (0.06)
n-nonanol	-[d]	0.78 (0.13)	-0.11 (0.08)
Dichloromethane	9.08 (20°C)	0.25 (0.1)	-0.61 (0.19)
n-octanol	10.30 (20°C)	1.05 (0.03)	0.02 (0.01)
n-heptanol	-[d]	1.58 (0.03)	0.20 (0.01)
n-hexanol	13.30 (25°C)	2.23 (0.05)	0.35 (0.01)

[a] Condition: between non-aqueous phase and 0.01 M phosphate buffer pH 7.4 at 30 ± 1°C and 24 h equilibrium

[b] not be able to calculated

[c] Wester, 1985

[d] No information

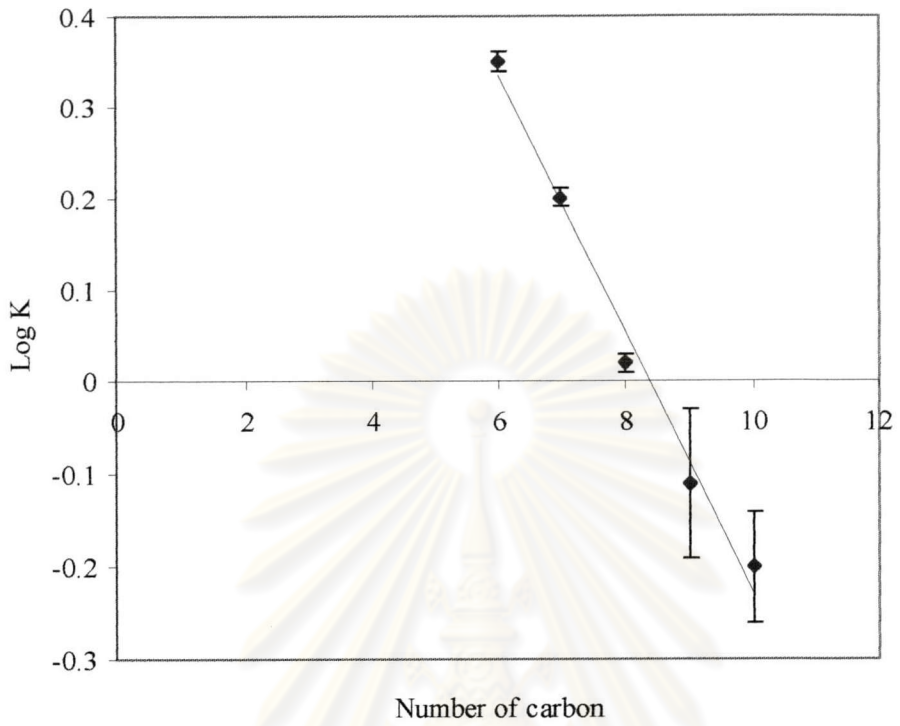

Figure 9 log K_{app} of AZT versus number of carbon atom in alcoholic solvents (n=3, error bar = SD).

2. Preformulation study of AZT

2.1 Solubility characteristic of AZT in variety of solvent systems

The solubilities of AZT in various solvents are displayed in Table 14

Table 14 Solubility studies of AZT by non-equilibrium method at 30 ± 1°C (n=3)

Polarity	Solvents	Dielectric constant (ε)	AZT Solubility	
			Volume (mcl)/10mg of AZT	Conc. (mg/ml)
Non polar	mineral oil	2.1 [a]	5000 (not soluble)	<2
	silicone	2.2[b]	5600 (not soluble)	<1.9
	isopropyl myristate	3.3[c]	5000 (not soluble)	<2
Semi polar	PEG 400	12.4 [d]	150	66.7
	Isopropyl alcohol	18.3[e]	650	15.4
	Ethanol	24.3 [a]	200	50
	Propylene glycol	32.0 [a]	1000	10
	n,n-dimethylacetamide	37.8 [d]	100	100
	DMSO	46.68	50	200
polar	water	80.4[a]	1000	10

[a] From the pharmceutical codex principles and practice of pharmaceutics 12[ed] 1994

[b] From AST instrument inc.

[c] From Harada,2000

[d] From the U.S. Nation Bureau of Standard Circular 514

[e] From Martin,1993 p.8

These solvents were classified according to their dielectric constants (ε) into non -polar solvent (ε ≅ 2-3), semi-polar solvent (ε ≅ 12-46), and polar solvent (ε ≅ 80) (Martin, 1993). According to Table 14, AZT can be best solubilized in DMSO to obtain the concentration of 200 mg/ml and the least solubilized solvent for AZT was those non polar solvents that only less than 2 mg/ml of AZT concentration can be observed. This solubility characteristics of AZT confirms again that it is very weakly acidic and non-ionizable compound. Eventhough AZT can be well dissolved in n,n-dimethylacetamide and DMSO, these two solvents are too toxic to be used in large amount for transdermal preparation.

These AZT solubility informations obtained could be applied for further mixed or combined solvent study in enhancing AZT solubility and reducing toxicity of each solvent in exposing to skin.

2.2 Determination of appropriate combination of vehicles for AZT

In this study, two solvents from Table 6 were selected to be binary vehicles such that the solubility of AZT should be increased. Since water is the most polar solvent that could not well dissolve AZT, in combining with other semi-polar like ethanol and IPA, the solubilities of AZT could be increased as displayed in Table 15 due to ethanol and IPA could dissolved AZT better than water. In the contrary to PEG 400, as incorporate water to PEG 400, the solubility of AZT was decreased almost 3 times. Because IPM could not miscible in water, IPM and ethanol were then combined as binary vehicles that can produce almost forty-time solubilization of AZT. This clearly indicates the very insoluble of AZT in this non polar solvent.

Table 15 Solubility determination of AZT by equilibrium method

Vehicle	Calc. ε	Solubility (mg/ml) (SD) (n=3)
Water	80.4	30.80 (0.53)
Ethanol	24.3	77.63 (0.59)
Ethanol : Water (V/V) 50 : 50 (F1)	52.35	158.64 (0.58)
IPA	18.3	42.78 (0.69)
IPA : Water (V/V) 50 : 50 (F2)	49.35	208.28 (0.22)
PEG 400	12.4	150.65 (0.39)
PEG 400 : Water (V/V) 50 : 50 (F3)	46.40	52.55 (0.29)
IPM	3.3	0.36 (0.01)
Ethanol : IPM (V/V) 50 : 50 (F4)	13.81	40.09 (0.44)

The solubility of AZT in IPA/water (F2) (208.28 mg/ml) and ethanol/water (F1) (158.64 mg/ml) are better than in PEG 400/water (F3) (52.55 mg/ml) and ethanol/IPM (F4) (40.09 mg/ml). Although, IPA/water, ethanol/water, and PEG 400/water contain the closely related dielectric constant (ε = 49.35, 52.35, 46.40). In the case of PEG 400/water and ethanol/water, it was observed that, the solubilities of AZT in PEG 400/water and ethanol/IPM (ε =13.81) are not different. These can explained that the total energy (or total force) for AZT solubilities in PEG 400/water and ethanol/IPM were similar. According to three steps of the solubility process, the total energy required for solubility of solute is as follow:

$$W = W_{22} + W_{11} - 2W_{12} \quad \text{.....(15)}$$

where W is the total energy for solubility of solute; W_{11} is the energy of creation of a hole in the solvent; W_{22} in the energy of interaction between solute molecules. (Martin, 1993).

However, the energy of AZT with PEG 400/water was also high due to hydrogen bonding between AZT and water. The energy of creation of a hole in PEG 400/water binary solvent was high too. On the other hand, the energy of AZT with ethanol/IPM was also low due to hydrophobic properties of IPM. The energy of creation of a hole in ethanol/IPM binary solvents was low too. Therefore, the above reason could lead to comparable solubility for both systems.

In these screening formulas, only 70% of saturated AZT was employed, although the maximum thermodynamic activity in these systems was not maintained.

This was just only to prevent seeding of drug crystals that could induce the faulty results. Solubility of AZT in phosphate buffer saline pH 7.4 at 33 ± 1°C was determined in order to plan for appropriated sampling times; it was 32.56 (0.02) mg/ml.

The AZT concentrations at 70% saturation as donor solution and permeation parameter are shown in Table 16. F4 gave the highest lag time for AZT permeating across newborn pig skin. Meanwhile, the lag time of F1, F2, and F3 formulations are identical due to the similar hydration effect of water to the stratum corneum. Moreover, flux of AZT from F4 is the highest while F1 and F2 have similar value.

The F3 formulation has higher flux more than those of F1 and F2. The permeability coefficients of AZT from F1 and F2 formulations are the lowest value. These could be attributed to either low partition coefficient and/or diffusion coefficient of drug through the skin. Permeability coefficient, K_p, of F3 formulation was 0.42×10^{-3} (cm/h) and F4 was 6.60×10^{-3} cm/h. However, the sampling times for these in vitro permeation studies are too short (12 h) to obtain steady-state especially for F4. Therefore, its permeation result was calculated by using initial flux.

In general there are three pathways postulated for the diffusion of solutes through the stratum corneum: transcellular, intercellular and transappendageal (sweat duct, follicular route). Since, the major pathway for transporting the water-soluble molecule is transcellular. The hydrophilic molecule is therefore poorly transported through the skin. However, hydration of the stratum corneum is somewhat important to determine the extent of absorption. By increasing the hydration, the resistance of the layer is decreased, presumably by causing a swelling of the compact structures in the horny layer (Florence and Attwood, 1998, Michael and Sheree, 2002).

Table 16 Permeation of 70% saturated AZT in binary vehicles across newborn pig skin

Binary Vehicle (50/50)	AZT solubility (SD) (mg/ml) (n=3)	AZT concentration at 70% saturation (mg/ml)	Lag Time (SE) (h) (n=5)	Flux (SE) (mcg/cm^2)/h (n=5)	Permeability (K_p) x 10^3 (SE) (cm/h) (n=5)
Ethanol/Water (F1)	158.64 (0.58)	111.04	2.86 (0.29)	9.96 (0.63)	0.09 (0.01)
IPA/Water (F2)	208.28 (0.22)	145.81	3.90 (0.09)	10.35 (0.67)	0.07 (0.08)
PEG 400/Water (F3)	52.55 (0.29)	36.80	3.29 (0.13)	15.52 (0.60)	0.42 (0.02)
Ethanol/IPM (F4)	40.09 (0.44)	28.05	8.64 (0.11)	185.23[a] (10.05)	6.60 (0.33)

[a] initial flux

F1, F2, and F3 contained water in the formula; consequently AZT and polar solvent penetration should be enhanced by hydration effect. For ethanol and IPA, they are alkanol which are different in only one carbon atom. These polar solvents are capable to partition into stratum corneum and diffused through out. The possible mechanism of action of the polar solvent like alcohol. It can insert into polar heading group regions causing "fluidization" by loosening the packing structure (Menon, Lee and Roberts, 1998). In this case AZT can permeate through the skin by convection with these polar solvents as indicated by the similar flux and permeability coefficient of F1 and F2. From the above, the concentration gradient had little effect to the drug transport (Table 16).

PEG 400, which is the hydrophilic polymer can not readily penetrate the skin. By combining PEG 400 with water as binary vehicle (F3), it can be partitioned and diffuse into skin. From chemical moiety, both polar ends of PEG polymer can be inserted between polar head of lipid bilayer. In addition, the long chain of oxyethylene group possibly inserts into hydrophobic chain of lipid. Then the loosening of lipid bilayer of stratum corneum could occured (Figure 10). In this case, the combine effect of PEG 400 and water enhance AZT penetration through the skin. This leading to the higher, K_p value of F3 (0.42×10^{-3} cm/h) than F1 (0.09×10^{-3} cm/h) and F2 (0.07×10^{-3} cm/h).

For ethanol/IPM (F4) binary system, the longest lag time was observed. The hydration effect of this binary vehicle is should be low and much less than the others. This causes the long time for AZT penetration and cumulation into stratum corneum. At steady state, AZT has constant flux through skin.

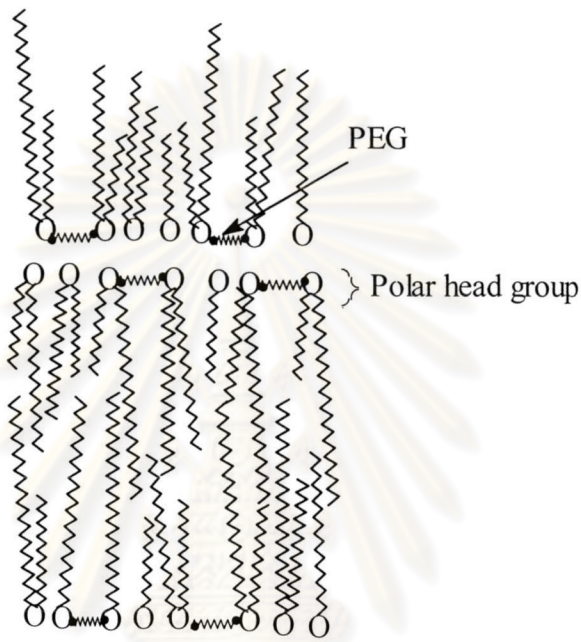

Figure 10 Diagrammatic representation of the possible mechanism of PEG 400

Many researchers have investigated the mechanism of the enhancing effect of ethanol on skin permeability (Ghaneum *et al.,* 1987; Berner *et al.*, 1989; Knutson *et al.*, 1990 and Hatanaka *et al.*, 1993). In the case of IPM, a non polar with low viscosity (5-6 mPas) solvent, has solubility parameter (δ) of 8.5 $(cal/cm^3)^{1/2}$ which is closely to stratum corneum (δ = 10 $(cal/cm^3)^{1/2}$ (Kibbe, 2000a). IPM can penetrate into skin and inserted between tail of hydrophobic lipid bilayer regions causing "fluidization" by loosening the lipid alkyl structure. The synergistic effect of ethanol as a hydrophilic vehicle and of IPM as a hydrophobic vehicle was also observed in this study.

Although transdermal delivery of AZT for the treatment of AIDS offers more advantages than conventional oral or IV administration, the high dose requirements of AZT presents a major challenge. Therefore, as a first step to developing a transdermal delivery system of AZT, an attempt to maximize the in vitro skin permeation rate (flux) of AZT was conducted. The calculated target flux from eqn.14 in Section 2.3 was 208 $mcg/cm^2/h$. Since the maximum flux obtained (Table 16) was only 185.23 $mcg/cm^2/h$, any preformulated AZT with these binary vehicles could not achieved this flux value. However, from this preliminary study, the ethanol/IPM binary vehicles was selected for further preformulated AZT study due to this binary vehicles gave the highest flux of AZT.

2.3 Preformulation of AZT in suitable binary vehicles

2.3.1 Determination of the appropriate volume ratio for ethanol/IPM binary vehicles

The mean permeation profiles of saturated AZT in ethanol/IPM (F5-F7) at three different volume ratios are given in Figure 11. These profiles have different lag time and slope. Each permeation profile clearly indicates two-different mechanisms on AZT permeation through newborn pig skin. Based on the aforementioned effect of binary vehicle on stratum corneum, it will take time for AZT to partition and diffusion through the skin in the first period. During this period, AZT flux was not constant until the stratum corneum was saturated by AZT. In the second period, the saturated AZT diffuse continuously and the steady-state permeation rate is reached.

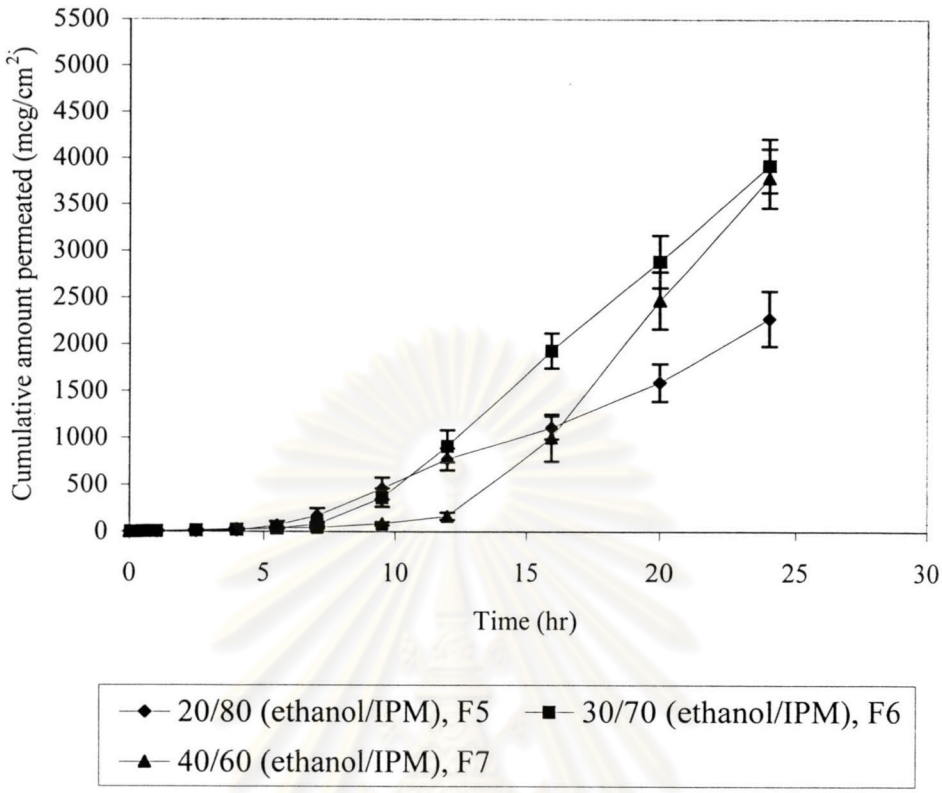

Figure 11 Permeation profiles of AZT from F5, F6 and F7 across newborn pig skin at 37 ± 1° C.

Donor solution is saturated with AZT in various compositions of ethanol/IPM binary vehicle (n=5, Error bar = SE).

The solubility and the corresponding permeation parameters of AZT from F5-F7 formulas were calculated and summarized in Table 17. The relationship between volume ratio of ethanol in binary vehicle and solubility, lag time, flux, and permeability coefficient (Kp) are given in Figure 12.

The solubility of AZT increased as the volume ratio of ethanol increased. This indicates the increasing solubility of AZT in ethanol.

F5, F6 and F7 showed the significant long lag time for the permeation of AZT ($p<0.05$) that F5 vs F6 vs F7 are significant different. The lag time increased in the direct proportion to ethanol giving the linear correlation ($r = 0.923$, $p<0.01$). For ethanol volume ratio of 40, the lag time of 13.11 h is not appropriate for transdermal preparation.

The flux values for AZT are also significantly different ($p<0.05$) among three formulations. The flux value was directly related to the volume ratio of ethanol (Figure 12c) ($r = 0.965$, $p<0.01$). Only F6 and F7 formulations gave the higher fluxes than the targeted flux (208 mcg/cm^2/h). Nevertheless, the permeation coefficient values for AZT are not statistically significant difference among them ($p >0.05$) (Figure 12d).

Table 17 Permeation of saturated AZT in different volume ratios of ethanol/IPM across newborn pig skin

Ethanol / IPM Ratio (V/V) (Formulation)	AZT Solubility (SD)(mg/ml) (n=3)	Lag Time (SE) (h) (n=5)	Flux (SE)(mcg/cm^2)/h (n=5)	Permeability (K_p) x 10^3 (SE) (cm/h) (n=5)
20/80 (F5)	9.61 (0.14)	6.10 (0.40)	120.69 (12.71)	12.64 (1.33)
30/70 (F6)	19.85 (0.25)	8.23 (0.44)	246.16 (14.64)	12.53 (0.74)
40/60 (F7)	26.22 (0.24)	13.11 (0.64)	348.02 (9.05)	12.68 (0.33)
F-Test	-[a]	S ($p<0.05$)	S ($p<0.05$)	NS ($p>0.05$)
Follow up using LSD	-[a]	F5: F6*, F7*	F5: F6*, F7*	-
Corelation test (r)	-[a]	0.923 ($p<0.01$)	0.965 ($p<0.01$)	0.010 ($p<0.01$)

[a] not applicable

* significant at level 0.05

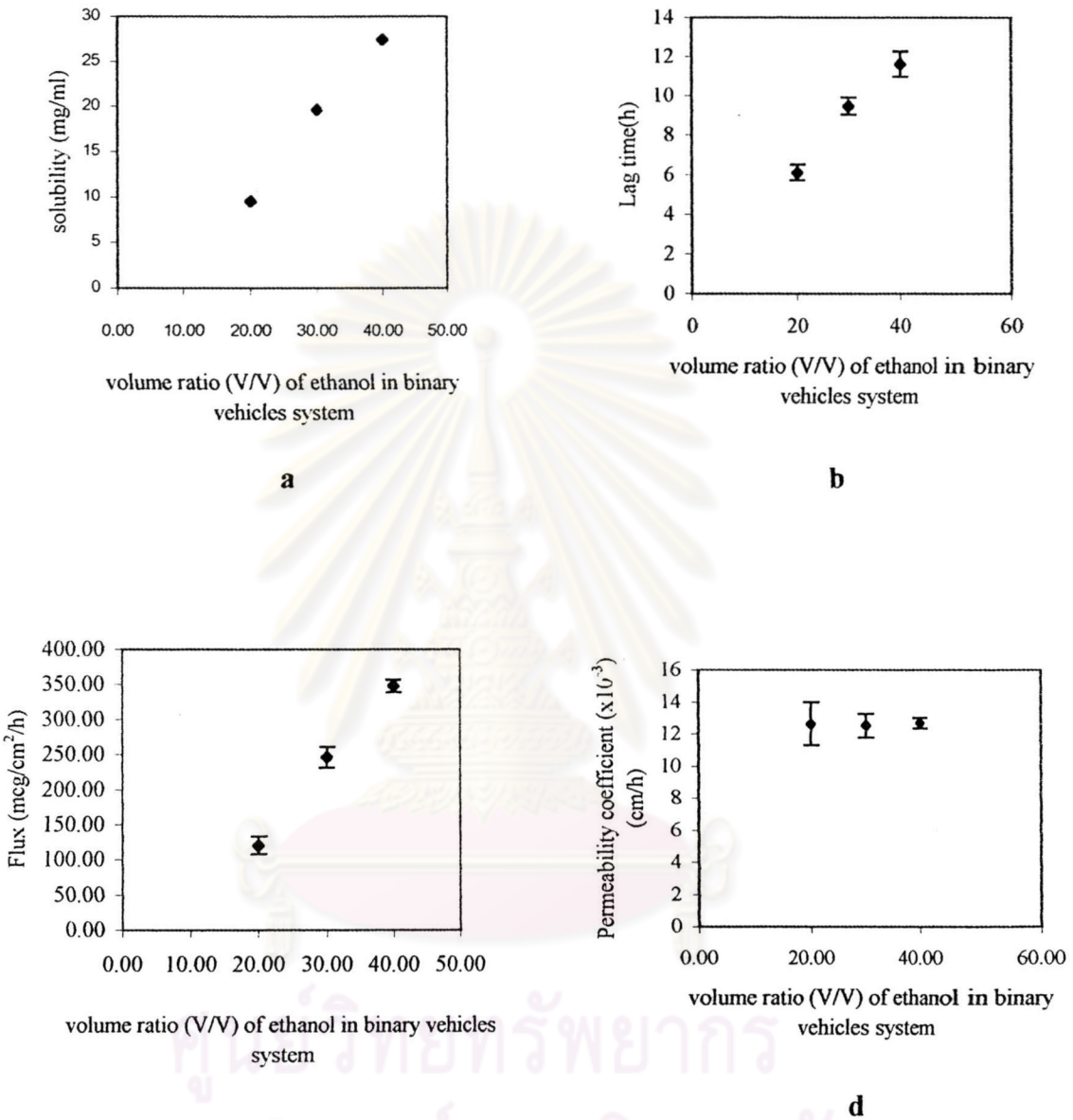

Figure 12 The relationship between the volume ratio (V/V) of ethanol in binary vehicles and (a) solubility, (b) lag time, (c) flux, (d) permeability coefficient of AZT saturated in different volume ratios of ethanol/ IPM across newborn pig skin.

The increase in the flux value of AZT as the volume ratio of ethanol increase can be explained in the term of AZT solubility. The more ethanol in the formulation, the more soluble of AZT becomes. Thus, the flux of AZT can be correlated to the saturated concentration of AZT as shown in Figure 13 ($r = 0.964$, $p<0.01$).

Even though the flux value varied among different volume ratios of ethanol/IPM, the permeability coefficients (K_p) were not quite different. This can be explained according to Figure 13 and eqn.13 ($K_p = J_{ss}/C_d$).

Furthermore by considering the definition of permeability coefficient (K_p), that $K_p = KD/h$ (from eqn.6), the diffusion coefficient (D), and skin/vehicle partition coefficient (K) are all included. In this study K_p are not different among the vehicles studied. Therefore, the unchanged K_p can be explained by effect of those previous parameters. However, besides the concentration effect as reported earlier, the increase in flux by increasing partition coefficient (K), when increasing the amount of ethanol cannot be ruled out. This as already shown in Table 17 the lag time was increased as the volume ratio of ethanol increased. It mean diffusion coefficient in K_p term decreased due to long lag time, in order to counteract and maintain K_p to be constant value, then partition coefficient (K) should be increased if the thickness of the skin is unchanged.

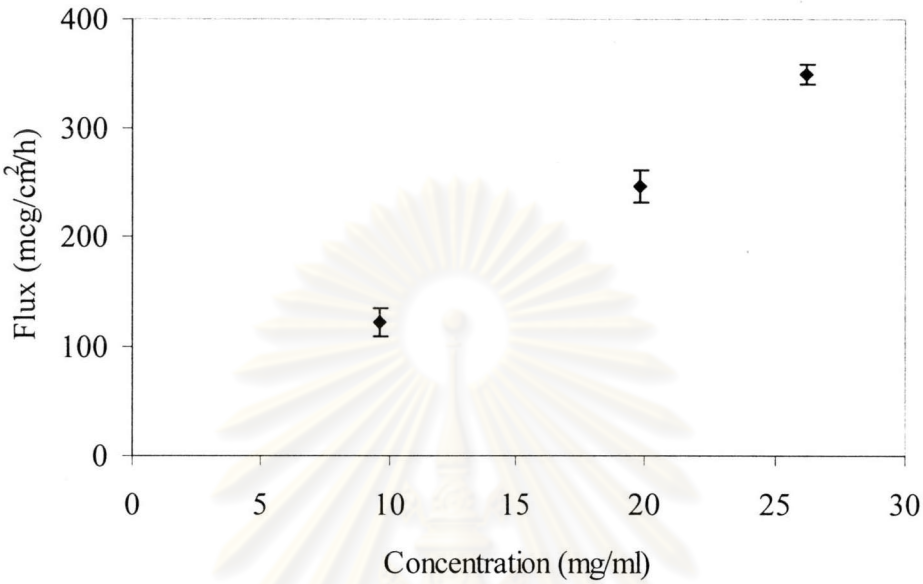

Figure 13 Correlation between concentration of AZT in F5-F7 and flux (pearson correlation; $r = 0.964$, $p<0.01$); error bar = SE

The synergistic effects of ethanol/IPM for enhancing AZT permeation were described in the previous study. Ethanol is miscible with water, so it can pull the water from corneocytes. When corneocyte lose water, the hydration effect was reduced. From this phenomenon, AZT need more time for being saturated in stratum corneum as the volume ratio of ethanol increase. Ethanol is also known to extract stratum corneum lipid and alter the barrier property, inducing high flux at higher ethanol content. This phenomenon is in agreement with what reported earlier (Kim *et al.,* 1992). Therefore a volume ratio at 50/50 is abandoned from the study.

On the other hand, IPM is an emollient by reducing the loss of water. The lag time was then decreased as volume ratio of IPM increased. In addition, the decrease of the lag times was also explained as the increasing of the diffusion of hydrophilic drug (Lee *et al.,* 1993; Kim and Chien, 1996; and Jin *et al.*, 1996). In this experimental study, very small drop of water was observed to appear on epidermis of newborn pig skin after 4-5 h of permeation study. It could possibly be the water from receiver compartment of the diffusion cell that reverse flux into donor by shunt partway (hair follicle of pig skin). These drops of water were immiscible with ethanol/IPM binary vehicle so the hydration effect of stratum corneum could be induced. This phenomenon will not observed if donor solution contains vehicle miscible with water. This occurrence could also imply an occlusion effect that seems like sweating out from hair follicles.

In the next study, ethanol/IPM (40/60), F7, was withdrawn because of its long lag time. The appropriate volume ratios of ethanol/IPM from this study were 20:80 (F5) and 30/70 (F6) as candidate formulation for the further study. However, The ethanol at low concentration can physical perturbation of lipoidal barrier region

of the stratum corneum. Therefore, the minimum of volume ratio of ethanol at 20/80 was selected for the Section 2.3.2.

2.3.2 Determination of the appropriate binary vehicles for AZT preformulation

Figure 14 represents permeation profiles of AZT with the permeation parameters are displayed in Table 18. All of the profiles showed the lag time of more than 5 h. At 24 h, F5 gave the highest cumulative amount AZT permeated through pig skin of approximately 2000 mcg/cm^2, while the cumulative amount of AZT from the others are only about 1000-1500 mcg/cm^2.

As shown in Table 18, the polarity indexes of hydrophobic vehicles do not correlate with AZT solubility. This informs the dependence of AZT solubility in these binary systems upon several factors such as molecular structure of hydrophobic solvent, inter-force between binary vehicle molecule, inter-force between vehicle and AZT molecule, etc.

The lag time for AZT permeation was classified into 2 groups. The first group is the lag time of AZT from F5, F8 and F10, these lag times are not statistically significant different ($p>0.05$). For the other group F9 and F11, the longer lag times for AZT were observed, which corresponded to 10.36, and 10.87 h, respectively. They are also not statistically significant difference ($p>0.05$).

MCT in F9, is the medium chained triglyceride, consists of a mixture of exclusively short or medium – chained triglycerides of fatty acids octanoic (caprylic) acid and decanoic (capric) acid. It has molecular weight of 500-600, viscosity of 25-

33 mPas (Kibbe, 2000). ADI in F11, is the hexanedioic acid diotyl ester, has molecular weigh of 370.5, viscosity of 15 mPas, solubility parameter of 8.7 $(cal/cm^3)^{1/2}$ (Aldrich, 1999).

Reminding again that, for very hydrophilic drug like AZT simple approach cannot be utilized for enhancing the drug transport through the skin. The solvent system which can react with stratum corneum, increase drug partition, clear the polar pathway, etc can lead to the successful drug transport. The evidence of the long lag time for AZT in F9 and F11 would be due to the high molecular weight and high viscosity of both compounds. This indicated that the viscosity of MCT or ADI changed the fluidity of microenvirontment of stratum corneum. In addition MCT and ADI can protect ethanol from reacting with the skin, resulted in prolonging the lag time.

The flux of AZT from F5 was statistically significant difference from F8, F9, and F10 ($p<0.05$). While, F11 give AZT flux significant difference from F8 and F10 ($p<0.05$). The flux from F5 (120.69 $mcg/cm^2/h$) and F11 (105.74 $mcg/cm^2/h$) are also statistically insignificant from each other ($p>0.05$). The value of AZT flux from F5 (120.69 $mcg/cm^2/h$) was influenced by the obviously high K_p value (12.64 $x10^{-3}$ cm/h). In the case of F11, the high permeated drug concentration (23.69 mg/ml) seem to be a major effect on flux or perhap high partition as may be seen from a long lag time of almost 11 h.

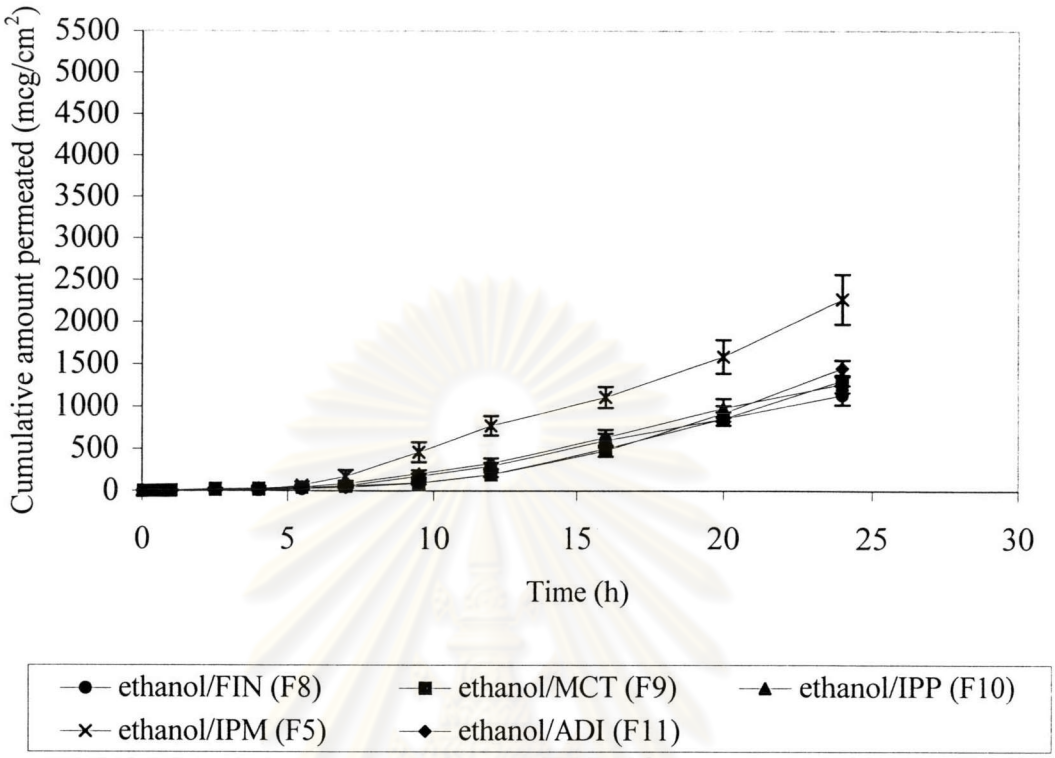

Figure 14 Permeation profiles of AZT from F5, F8, F9, F10, F11 across newborn pig skin at 37± 1°C.

Donor solution is saturated with AZT in each individual ethanol/ hydrophobic (20/80) binary vehicles system (n=5, error bar = SE). FIN = C_{12-15} alkyl benzoate; MCT = medium chain triglyceride; IPM = isoprpyl myristate; IPP = isopropyl palmitate; ADI = dioctyl adipate

Table 18 Permeation parameters of saturated AZT in ethanol/several hydrophobic (20/80) binary vehicles across newborn pig skin

Formulation	Polarity Index (mN/m)[a]	AZT Solubility (SD) (mg/ml) (n=3)	Lag Time (SE) (h) (n=5)	Flux (SE) (mcg/cm^2)/h (n=5)	Permeability (K_p) x 10^3 (SE) (cm/h) (n=5)
ethanol/FIN, (F8)	18.8	17.15 (0.36)	7.25 (0.59)	67.50 (6.38)	3.95 (0.37)
ethanol/MCT, (F9)	20.2	19.62 (0.19)	10.36 (0.57)	92.82 (5.06)	4.75 (0.26)
ethanol/IPM, (F5)	24.3	9.61 (0.14)	6.10 (0.40)	120.69 (12.71)	12.64 (1.33)
ethanol/IPP, (F10)	25.2	11.59 (0.67)	7.25 (0.89)	75.62 (6.28)	6.50 (0.54)
ethanol/ADI, (F11)	27.0	23.69 (0.42)	10.87 (0.27)	105.74 (6.01)	4.50 (0.26)
F-Test	-	-[b]	S ($p<0.05$)	S ($p<0.05$)	S ($p<0.05$)
Follow up using LSD	-	-[b]	F: F8*, F5*, F10* F11: F8*, F5*, F10*	F5: F8*, F9*, F 10* F11: F8*, F10*	F5: F8*, F9*, F10*, F11*

[a] Polarity Index = Interfacial tension between oil and water (ICI surfactants at the interface of ideas and success)
[b] not appllicab
* significant at level 0.05

F5 showed the highest K_p value (12.64 x 10^{-3} cm/h) that is statistically significant difference from the others ($p<0.05$). The K_p values from the other formulations are not statistically significant difference ($p>0.05$). This confirms that IPM in F5 is the most effective vehicle for AZT permeation.

The capacity of hydrophobic vehicles for enhancing AZT permeation could be implied from the K_p value.

Hydrophobic vehicles in this study can induce AZT permeation when they are combined with ethanol. The mechanism of synergistic effect of these binary vehicles from occlusion and fluidization was clearly explained. However, the effect of hydrophobic vehicles for inducing AZT permeation are different due to their chemical characters. The chemical characters of hydrophobic vehicles are shown in Figure 15.

Vehicle :	FIN	MCT	IPM	IPP	ADI
MW :	266.1-302.1	500-600	270.51	298.51	370.5
Viscosity :	13	25-33	5	8	15

Figure 15 Chemical properties and molecular shape of various hydrophobic vehicles in this study.

Three factors could affect on AZT permeation. They are molecular weight, viscosity and molecular shape (for creating the disorientation in lipid bilayer) of hydrophobic vehicle. Rotational freedom of alkyl chain in the intercellular lipid lamellae of the stratum corneum due to hydrophobic repulsion force allows a greater mobility of the hydrocarbon chains that may result in enhancing diffusivity of solute. This could be induced by molecular shape interaction (Walter, 2002).

Therefore, the highest K_p value of AZT from F5 should be resulted from the chemical properties of IPM those are appropriate for inducing AZT permeation. IPM is a low molecular weight compound (270.51) with low viscosity (5 mPas), and appropriate shape.

Figure 15 shows the different molecular shape of these hydrophobic vehicles. It is interesting to observe that even if the molecular weight and viscosity of IPM and IPP are similar, the K_p and flux values of AZT using IPM are approximately 51 and 62 % higher than IPP, respectively ($p<0.05$). In contrast, the driving force of the system containing IPP is higher. For the lag time values, they are nearly the same ($p>0.05$) between IPM and IPP. Therefore, it can be speculated that driving force, different in diffusion of permeated AZT through the totursity of the skin through transcellular should be ruled out. The major mechanism probably comes from the molecular shape of IPM that can be appropriately inserted into alkyl carbon of lipid bilayer and created free volume more than IPP due to suitable molecular configuration arrangement of IPM molecule. In addition, FIN, MCT, and ADI showed the K_p value less than that from IPM due to the polar head of these solvents are larger and inappropriate to alter the lipid bilayer.

After comparative evaluation of the various parameters (Table 18.) ethanol and IPM dominantly affected the AZT transport through the skin. Although ADI in F11 show insignificant flux ($p>0.05$) from IPM in F5 but it give longer lag time. Therefore, IPM was selected to combine with ethanol for further study.

2.4 Study the addition of enhancers into preformulated AZT

The ethanol/IPM (20/80), F5, and ethanol/IPM (30/70), F6, were selected for adding enhancers as tabulated in Table 10.

2.4.1 Effect of NMP with binary vehicles on AZT permeation

The formulations F12, F13 and F14 were experimented comparing to F5. Figure 16 represents the permeation profiles of AZT obtained from formulations F5, F12, F13, and F14. Every permeation profile showed the lag time up to 6 h. Preformulated AZT containing 10% NMP (F14) showed the highest and cumulative amount of permeated AZT of more than 4500 mcg/cm^2 at 24 h. The formulation with 1% NMP (F12) seems to retard permeation of AZT while the F13 with 5% NMP response as if no NMP (F5) was added.

The permeability parameters of AZT are expressed in Table 19. As the percentage of NMP increased, the solubility of AZT was also increased. AZT can be more solubilized in the present of NMP because NMP can induce a certain degree of polarity in solvent molecules like ethanol which is semi-polar solvent. Since semi-polar compound may act as intermediate solvent to bring about miscibility of polar and non-polar liquids, the combinations of ethanol/IPM (20/80) and NMP can then produce great miscibility. Moreover, NMP is a strong proton acceptor capable to

form complex with hydrogen atom at carbonyl moiety of AZT. Therefore, AZT solubility was increased when the amount of NMP increased as described above.

The lag time of AZT in all these formulations showed approximately 6 h that were not significantly different from F5 ($p>0.05$). The microenvironment (such as fluidity of system) of stratum corneum was not quite changed with enhancer. Therefore, AZT still has to take time to permeate in the similar pathway of stratum corneum at non steady – state.

The flux of AZT from formulation F12, F13 and F14 were significantly different ($p<0.05$). Flux was increased when the amount of NMP increased. Formulation F14 with 10 % NMP in the binary vehicles showed the highest flux value of 284.92 mcg/cm^2/h. This flux value achieved to the proposed target flux (208 mcg/cm^2/h). However permeability coefficient K_p of AZT among of F12 - F14 formulas were statistically non-significant ($p>0.05$).

A possible mode of NMP action may involve the polar head region of the bilayer as ethanol (Yoneto *et al.,* 1995). There were no significant differences in K_p and lag time among F12-F14 ($p>0.05$). Therefore, fluxes of AZT from these formulas were increased by dominant concentration effect.

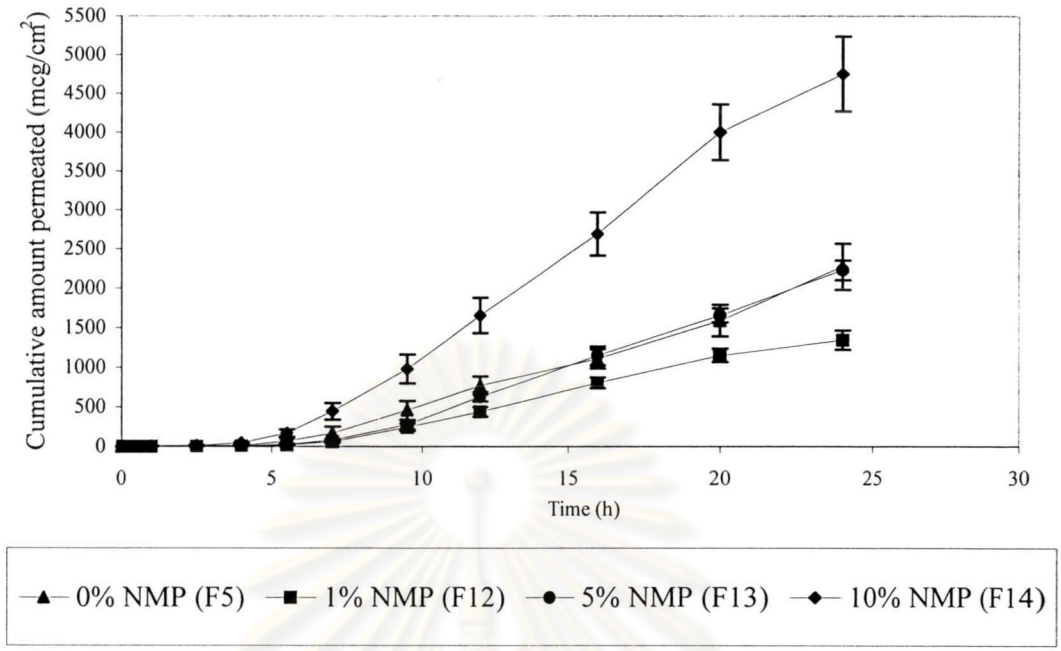

Figure 16 Permeation profiles of saturated AZT in ethanol/IPM (20/80) binary vehicles with 0%, 1%, 5%, 10% V/V of NMP (*N*-methyl-2-pyrrolidone) across newborn pig skin at 37 ±1°C (n=5, error bar = SE).

Table 19 Permeation parameters of saturated AZT in Ethanol/IPM (20/80) binary vehicles with and without NMP across newborn pig skin

Ethanol/IPM (20/80) + NMP (%V/V) (Formulation)	AZT Solubility (SD) (mg/ml) (n=3)	Lag Time (SE) (h) (n=5)	Flux (SE)(mcg/cm^2)/h (n=5)	Permeability(K_p) x 10^3 (SE)(cm/h) (n=5))
0% (F5)	9.61 (0.14)	6.10 (0.40)	120.69 (12.71)	12.64 (1.33)
1% (F12)	14.07 (0.46)	6.59 (0.35)	84.76 (5.62)	6.04 (0.40)
5% (F13)	27.50 (0.45)	6.97 (0.30)	128.34 (5.94)	4.65 (0.21)
10% (F14)	42.60 (0.49)	6.25 (0.45)	284.92 (18.34)	6.74 (0.43)
F - Test	-[a]	NS ($p>0.05$)	S ($p<0.05$)	S ($P<0.05$)
Follow up using LSD	-[a]	-	F5:F12*,F14*; F14:F5*,F12*, F13*	F5:F12*, F13*, F14*

* significant at level 0.05
[a] not applicable

However, the permeability coefficient values of formulations F12, F13, and F14 were less than two times of formulation F5 that contain no enhancer. The action of IPM at alkyl chain of lipid bilayer was reduced due to the replacement of NMP in these formulations. While the action of NMP at polar head of lipid bilayer was increased, it cannot counteract the disorientation effect of IPM on lipid bilayer. This evidence showed that AZT, in the formulation F12 – F14, prefer to locate at polar head region resulting the slower permeation of AZT through stratum corneum comparing to formulation F5.

2.4.2 Effect of oleic acid with binary vehicles on AZT permeation

As shown in Figure 17 the lag time of AZT is present at 4-6 h before it can permeate out and start to obtain steady – state flux.

The solubility of AZT increased from 9.61 mg/ml in ethanol/IPM (20/80) for F5 to 15.33 mg/ml when 5% V/V oleic acid was added into the formulation (F16). This combination of 5% oleic acid with binary vehicle that gave the highest solubility of AZT is the best among this group of study as indicated in Table 20. The solubility of AZT in IPM, oleic acid, and ethanol at 33 ± 1°C were reported to be 0.36, 1.99, and 77.63 mg/ml, respectively. Therefore, AZT was more soluble when oleic acid was added up to 5% by volume as formulated in F16. If oleic acid was added into the preformulation of AZT to 10% (F17), AZT was less soluble due to the increasing of hydrophobicity of this enhancer in the system.

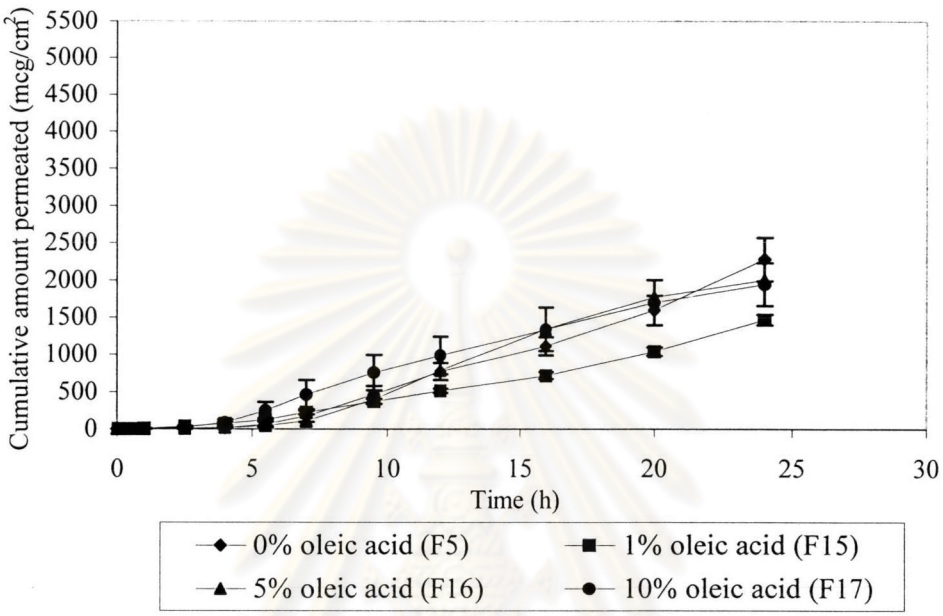

Figure 17 Permeation profiles of saturated AZT in ethanol/ IPM (20/80) with 0%, 1%, 5%, 10% V/V of oleic acid across newborn pig skin at 37± 1°C (n=5, error bar = SE).

Table 20 Permeation parameters of saturated AZT in Ethanol/IPM (20/80) binary vehicles with and without oleic acid across newborn pig skin

Ethanol/IPM (20/80) + oleic acid (%V/V) (Formulation)	AZT Solubility (SD) (mg/ml) (n=3)	Lag Time (SE) (h) (n=5)	Flux (SE)(mcg/cm^2)/h (n=5)	Permeability(K_p) x 10^3 (SE)(cm/h) (n=5))
0% (F5)	9.61 (0.14)	6.10 (0.40)	120.69 (12.71)	12.64 (1.33)
1% (F15)	10.35 (0.47)	4.24 (0.43)	69.12 (3.41)	6.71 (0.33)
5% (F16)	15.33 (0.29)	6.11 (0.32)	130.60 (6.04)	8.50 (0.39)
10% (F17)	9.58 (0.49)	5.37 (0.71)	88.60 (10.65)	9.16 (1.10)
F-Test	-[a]	S ($p<0.05$)	S ($p<0.05$)	S ($p<0.05$)
Follow up using LSD	-[a]	F15: 16*, F5* F5: F15*	F15: F16*, F17*, F5*; F16: F15*, F17*	F5: F15*, F16*, F17*; F15: F16*, F17*

[a] not applicable
* significant at level 0.05

The lag time of AZT from formulation F15 was significantly less than those from F16 and F5 ($p<0.05$), that was similar F17 ($p>0.05$). However, the lag time of AZT from F16 and F5 are statistically non-significant ($P>0.05$). This indicated that, 1% oleic acid, F15, can reduce lag time of AZT from 6.10 h to 4.24 h. It was concluded that both IPM (from result of 2.3.1) and oleic acid can reduce lag time of AZT. Oleic acid is an unsaturated fatty acid that generally uses as penetration enhancer. It has viscosity 26 mPas (Kibbe, 2000b). At an appropriate concentration oleic acid can synergies with IPM in reducing the lag time of AZT. If more oleic acid was combined in binary vehicle (ethanol/IPM), its viscosity may retard the partition of IPM and /or AZT itself from binary vehicle system to stratum corneum. Therefore, synergistic effect for reducing lag time of IPM was decreased.

The flux values of AZT from F15, F16 and F17 were significantly different ($p<0.05$). Formulation F16 shows the highest flux of 130.60 mcg/cm^2/h which would be affected by both AZT concentration and permeability coefficient. However, this flux value is not significant difference from that obtained in formulation F5 (without enhancer).

A K_p value of AZT from formulation F15 was statistically significance less than F16 and F17 ($p<0.05$) while F16 and F17 formulations gave the similar K_p values ($p>0.05$). However, these K_p values were less than the one from formulation F5. This implies the more influence of IPM than that of oleic acid on the K_p value of AZT. By comparing the comparative molecular structure of IPM and oleic acid for creating free volume in lipid bilayer. Molecular shape of IPM and oleic acid are as follows:

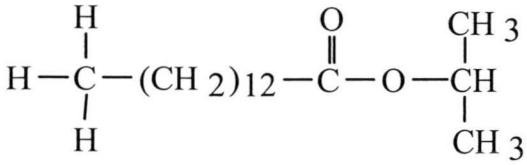

IPM

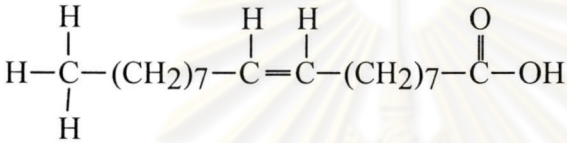

Oleic acid

Both IPM and oleic acid can physically disturb the lipid of the stratum corneum. IPM molecule may create more free space (free volume) in the intercellular lipid lamellae of the stratum corneum that allows the greater mobility of the hydrocarbon chain than oleic acid. This phenomenon is illustrated in Figure 18. Therefore, the velocity of AZT permeate through stratum corneum was slowly as compared with F5.

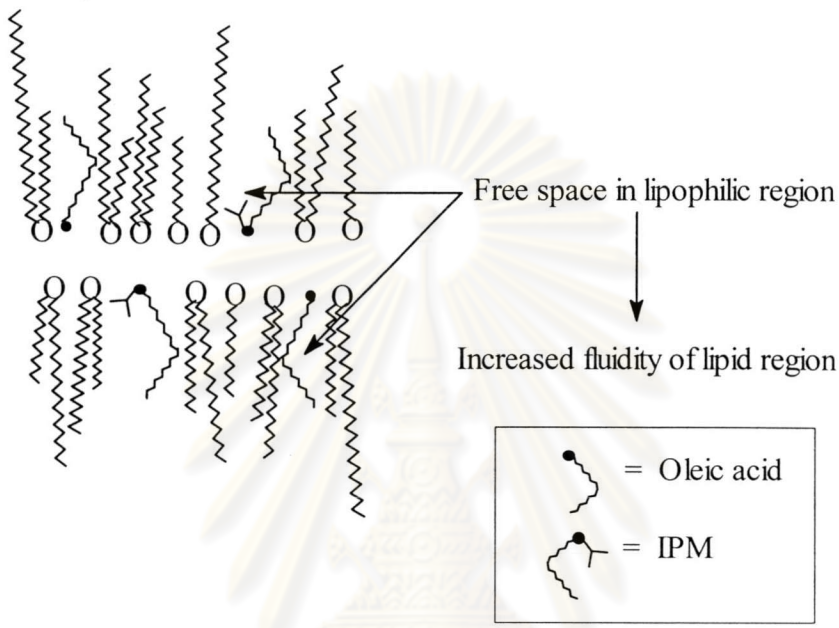

Figure 18 The propose mechanism of IPM and oleic acid in enhanced diffusivity.

2.4.3 Effect of lauric acid with binary vehicles on AZT permeation

The permeation profiles of AZT from formulation F5, F18, F19 and F20 are displayed in Figure 19. The permeation profiles of these formulations have lag time about 5 h before drug can permeate out to obtain steady-state flux.

The solubility, lag time, flux, and permeability coefficient of AZT in the presence of lauric acid are summarized in Table 21. The solubility of AZT in each formulation as mentioned before was different. The 5% lauric acid combined with binary vehicle was the best combination to solubilizing AZT. The reason for explaining the characteristic of AZT solubility in these formulations is quite similar to 2.4.2.

The lag time of AZT from formulation F18 was less than F19 ($p<0.05$). However, the lag time of AZT from F5, F19 and F20 are non significant ($p>0.05$). This indicated that 1% lauric acid, F18, can reduce lag time of AZT from 6.10 h to 3.32 h.

Lauric acid, which is a saturated fatty acid, is generally used as penetration enhancer. At an appropriate concentration, lauric acid can have synergistic effect with binary vehicle to reduce lag time. If more lauric acid combined in binary vehicle (ethanol/IPM), its viscosity retards partition of IPM or perhap drug from binary vehicle system to stratum corneum like oleic acid. Therefore, synergistic effect for reducing lag time of IPM was decreased.

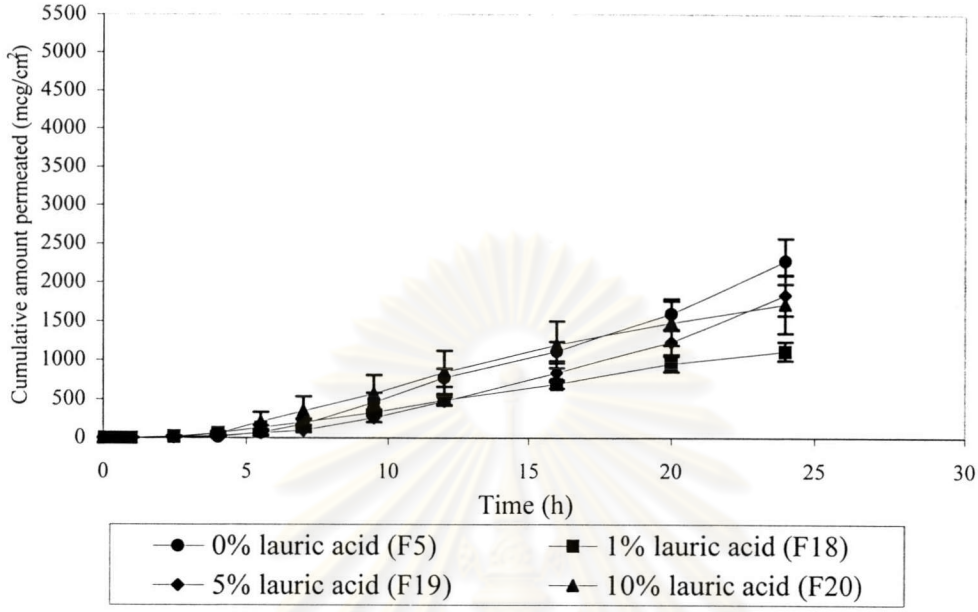

Figure 19 Permeation profiles of saturated AZT in ethanol/IPM (20/80) with 0%, 1%, 5%, 10% V/V of lauric acid across newborn pig skin at 37±1°C (n=5, error bar = SE).

Table 21 Permeation parameters of saturated AZT in Ethanol/IPM (20/80) binary vehicles with and without lauric acid across newborn pig skin

Ethanol/IPM (20/80) + lauric acid (%V/V) (Formulation)	AZT Solubility (SD) (mg/ml) (n=3)	Lag Time (SE) (h) (n=5)	Flux (SE)(mcg/cm^2)/h (n=5)	Permeability(K_p) x 10^3 (SE)(cm/h) (n=5))
0% (F5)	9.61 (0.14)	6.10 (0.40)	120.69 (12.71)	12.64 (1.33)
1% (F18)	10.25 (0.23)	3.32 (0.46)	54.78 (5.42)	5.32 (0.53)
5% (F19)	13.24 (0.34)	7.40 (0.61)	106.28 (13.60)	8.01 (1.15)
10% (F20)	9.38 (0.55)	5.48 (0.78)	93.11 (8.70)	9.99 (0.93)
F-Test	-[a]	S ($p<0.05$)	S ($p<0.05$)	S ($p<0.05$)
Follow up using LSD	-[a]	F18: F19* F5: F1*	F5: F18*; F18: F5*,F19*, F20*	F19: F5*, F18*; F5: F18*,F19*, F20*

[a] not applicable
* significant at level 0.05

The flux value of AZT from F18 was statistically significant less than F5, F19 and F20 ($p<0.05$). However, the fluxes from F19, F20 and F5 were not significantly different ($p>0.05$).

A K_p value of AZT from F19 found to be significantly different from F18 and F5 ($p<0.05$). However, these K_p values of F18, F19, and F20 were statistically significant less than without enhancer (F5).

The result of adding lauric acid as enhancer into the preformulated AZT was quite identical to the use of oleic acid (Table 20 and 21), although lauric acid is saturated fatty acid while oleic acid is unsaturated fatty acid. Hence, the permeation parameters of AZT when using either oleic acid or lauric acid as enhancer could possibly be explained in the same manner. The mechanism of permeation enhancement of lauric acid, saturated fatty acid, is similar to oleic acid (Francoeur *et al.,* 1990). Therefore, the reason of velocity of AZT permeated through the stratum corneum from F18-F20 is slower than F5 as described above.

Adding enhancer (hydrophilic or hydrophobic enhancer) in ethanol/IPM (20/80) can reduce K_p value when compared with no enhancer. However, 10% NMP (F14) in this binary vehicle has the highest flux (284.92 mcg/cm^2/h) which it achieve to target flux, while adding of oleic acid and lauric acid were not reach target flux. Therefore, F14 was candidate to study for evaluation of AZT transdermal delivery system.

Moreover, NMP was chosen for studying the effect of ethanol/IPM (30/70) binary vehicle with enhancer on AZT permeation in order to select the candidate formulation for evaluation of AZT transdermal delivery system.

2.4.4 Effect of ethanol/IPM (30/70) binary vehicle with NMP on permeation parameter of AZT

The NMP was selected from the previous study because of oleic acid and lauric acid can not obviously increase the flux of AZT. The F21-F23 were observed in this study.

Figure 20 represents permeation profiles of AZT from F6, F21-F23. These permeation profiles have similar lag time about 9 h after which AZT was permeated out. The slope of permeation profiles were increased when the percentage of NMP increased. The slope of F23 is the highest and cumulative amount permeated of AZT is about 8000 mcg/cm^2 at 24 h.

The solubility and the corresponding value of permeation parameters of AZT from F21-F23 formulation were calculated and summarized in Table 22. The relationship between the quantitative of NMP and solubility of AZT, lag time, flux, permeability coefficient are shown in Figure 21. The relationship between solubility of AZT in donor and flux is given Figure 22.

Solubility of AZT was increased as the percentage of NMP increased. This is because owing to NMP is good solvent as the results are summarized in Table 22 and Figure 21a.

In the case of lag time, it was observed that each formulation has long lag time about 7 h for the permeation of AZT and the lag time among these formulations are insignificant ($p>0.05$). Moreover, these lag times were not significantly different ($p>0.05$) which show in Table 22 and Figure 21b. Adding NMP into binary vehicles indicated that lag time do not change. It may be explained that, NMP was not

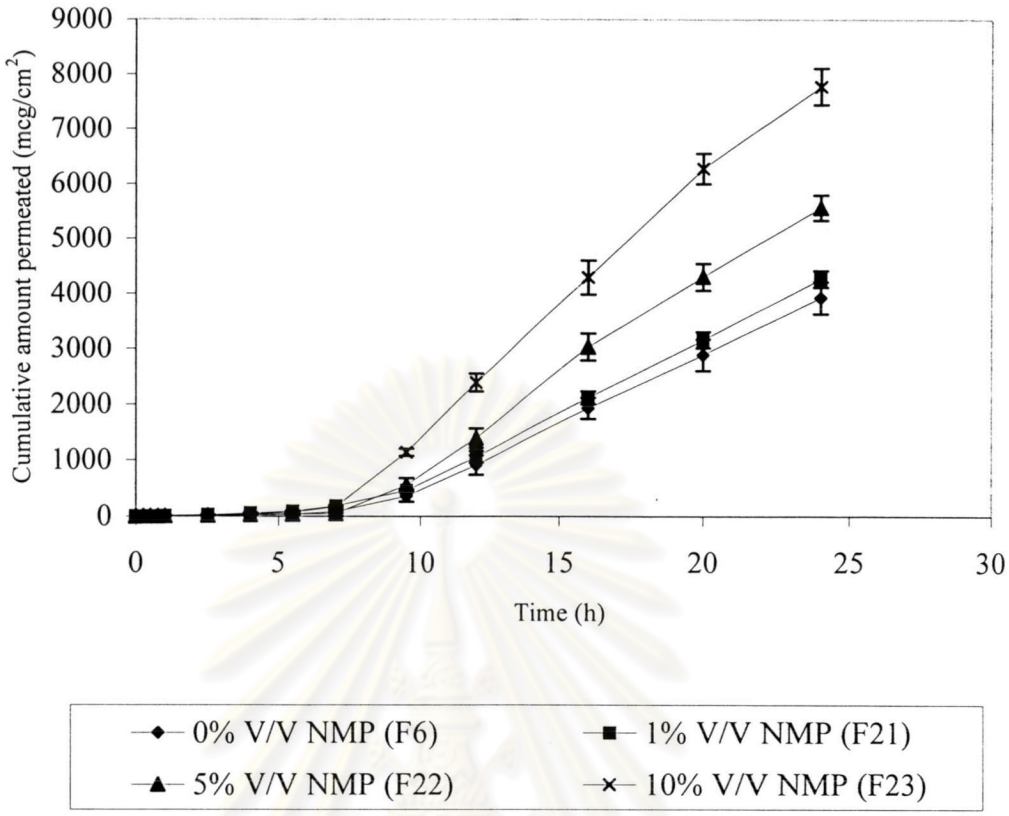

Figure 20 Permeation profiles of saturated AZT in ethanol/IPM (30/70) with 0%, 1% 5%, 10% V/V of NMP across new born pig skin at 37 ± 1°C (n=5).

Table 22 Permeation parameters of saturated AZT in Ethanol/IPM (30/70) binary vehicles with and without NMP across newborn pig skin

Ethanol/IPM (30/70) + NMP (%V/V) (Formulation)	AZTSolubility (SD) (mg/ml) (n=3)	Lag Time (SE) (h) (n=5)	Flux (SE)(mcg/cm^2)/h (n=5)	Permeability(K_p) x 10^3(SE)(cm/h) (n=5)
0% (F6)	19.85 (0.25)	9.47 (0.44)	246.16 (14.64)	12.53 (0.74)
1% (F21)	23.44 (0.43)	7.91 (0.55)	262.60 (9.99)	11.20 (0.43)
5% (F22)	33.37 (0.28)	7.80 (0.13)	348.84 (9.3)	10.46 (0.27)
10% (F23)	56.27 (0.19)	7.49 (0.59)	460.34(18.72)	8.16 (0.33)
F-Test	-[a]	NS ($p>0.05$)	S ($p<0.05$)	S ($p<0.05$)
Follow up using LSD	-[a]	-	F21: F22*, F23* F22: F21*, F23*, F6* F23: F6*, F21*, F22* F6: F22*, F23*	F21: F23* F22 : F23* F23: F21*, F22*, F6*
Correlation test (r)	-[a]	-	0.912 ($p<0.01$)	-

[a] not applicable
* significant at level 0.05

different change microenvironment (such as viscosity of system) of the toturisty of stratum corneum when compared with no enhancer. Therefore, AZT used time to permeate in the similar manner at non steady-state.

AZT flux from F21, F22, F23 formulations were also significantly different ($p<0.05$). The flux value was directly related to the percentage of NMP (Figure 21c) ($r = 0.912$, $p < 0.01$). Therefore, it can be speculated that NMP combined in ethanol/IPM (30/70) increase AZT solubility in the stratum corneum by increasing the driving force of AZT. These fluxes from F21, F22, and F23 were 262.60, 348.84, 460.34 mcg/cm^2/h, respectively. However, flux from F21 and F6 were insignificant different ($p>0.05$). Moreover, these fluxes achieve to target flux (208 mcg/cm^2/h).

The permeability coefficient, K_p, of 10% NMP in F23 was the lowest ($p <0.05$). While K_p values of F21, F22, and F6 (no enhancer) were not significant ($p> 0.05$). From Figure 21d, indicated that K_p was decreased by adding 10% NMP into ethanol/IPM (30/70) binary vehicle.

A possible mode of NMP action was described above. They were insignificant difference in K_p among F6, F21 and F22. Therefore, flux of AZT when increase NMP should flavor by dominant concentration effect. It was confirmed by correlation between solubility (as concentration in donor) and flux of AZT in Figure 22. This correlate is linear ($r = 0.944$; $p < 0.01$).

However, K_p value of AZT from F23 is different from those K_p values of F6, F21, F22 ($p <0.05$). The action of IPM at alkyl chain of lipid bilayer was reduced due to IPM was replaced by high percentage of NMP in the formulation. This effect was obviously observed at 10% NMP of F23. Moreover, the increasing NMP (10%

in ethanol/IPM; 30/70) could possibly form complex like hydrogen bonding with IPM so IPM was reduced action at alkyl chain of lipid bilayer.

From overall result of permeation parameters, F23 was candidated to study for evaluation of AZT transdermal delivery system due to it gave the highest flux.

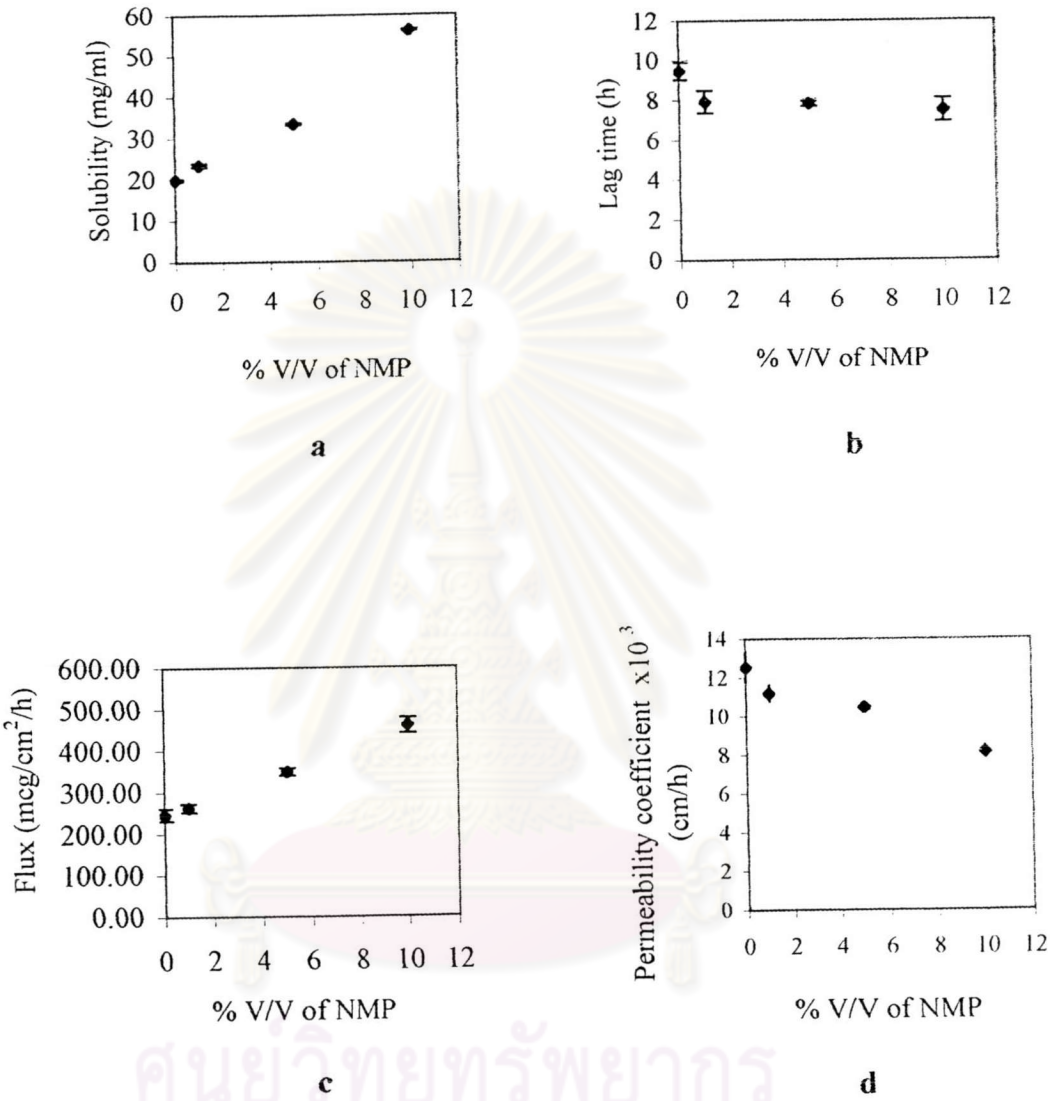

Figure 21 The relationship between the % V/V of NMP and (a) solubility, (b) lag time, (c) flux, (d) permeability coefficient of AZT saturated in ethanol/IPM (30/70) across newborn pig skin

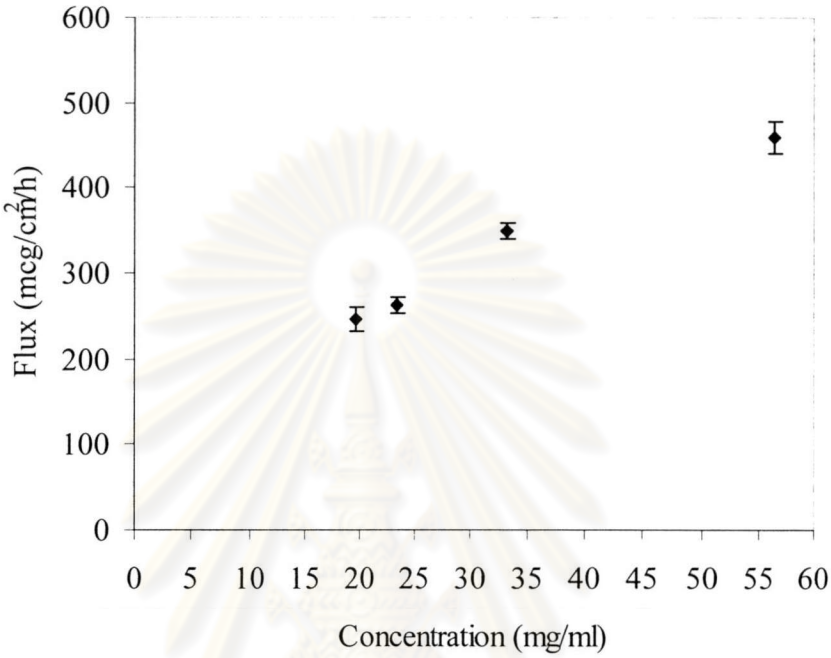

Figure 22 Correlation between concentration of AZT in F6, F21-F23 and flux (pearson correlation; $r = 0.944$, $p<0.01$)

3..Evaluation of AZT transdermal delivery system

The formulation of F14 (ethanol/IPM, 20/80) and F23 (ethanol/IPM, 30/70) were chosen from the previous study for investigation the effect of controlling membrane on AZT release and permeation.

3.1 Effect of controlling membrane on drug release study

F14 was chosen to represent as a candidate formula for this study. Figure 23 represents the comparative release profiles of AZT from F14 across microporous and nonporous membrane at 37 ± 1°C. For the release profile of AZT through polyethylene microporous membrane, it was observed that AZT release immediately and lag time was disappeared. This profile indicated that two difference mechanisms were obviously seen. In the first period shown a sharp left turn slop. During this period, the release of AZT had constant flux (0-0.75 h). Then the slope was decreased. The constant flux appeared again during the rage of 9.5-24 h in the second period. On the other hand, AZT could not transport through 9% ethyl vinyl acetate nonporous membrane.

The lag time, flux, and permeability coefficient were calculated and summarized in Table 23. Both of the release data had no lag time. In the range of 0-0.75 h, AZT had flux of 3951.27 mcg/cm^2 /h when it permeated through microporous membrane. AZT was released through microporous membrane, which might contain fluid-filled pore. In this case the AZT could diffuse instantaneously through the pores as observed by first steady state flux. AZT had flux of 68.47 mcg/cm^2 /h in the range of 9.5-24 h. Although, the sink condition was saved at all investigation time,

this flux was reduced about fifty times from the first period. IPM, the major component in formula, immiscible with water. When IPM released through microporous membrane, it cumulated under membrane until it equilibrium. Therefore, AZT was retarded release to receiving solution. On the other hand, AZT had flux of 1.40 mcg/cm^2 /h when it diffused through nonporous membrane (9% EVA) at the range of 0-24 h. This release profile is shown in Figure 24. The AZT release occurred by diffusing mechanism directly through the material of membrane. Moreover, the permeability coefficient of AZT permeation through microporous more than nonporous membrane about 2000 times at 0-0.75 h, and 40 times at 9.5-24 h. Therefore, nonporous membrane was not appropriated for developing AZT transdermal delivery because AZT poorly released through it.

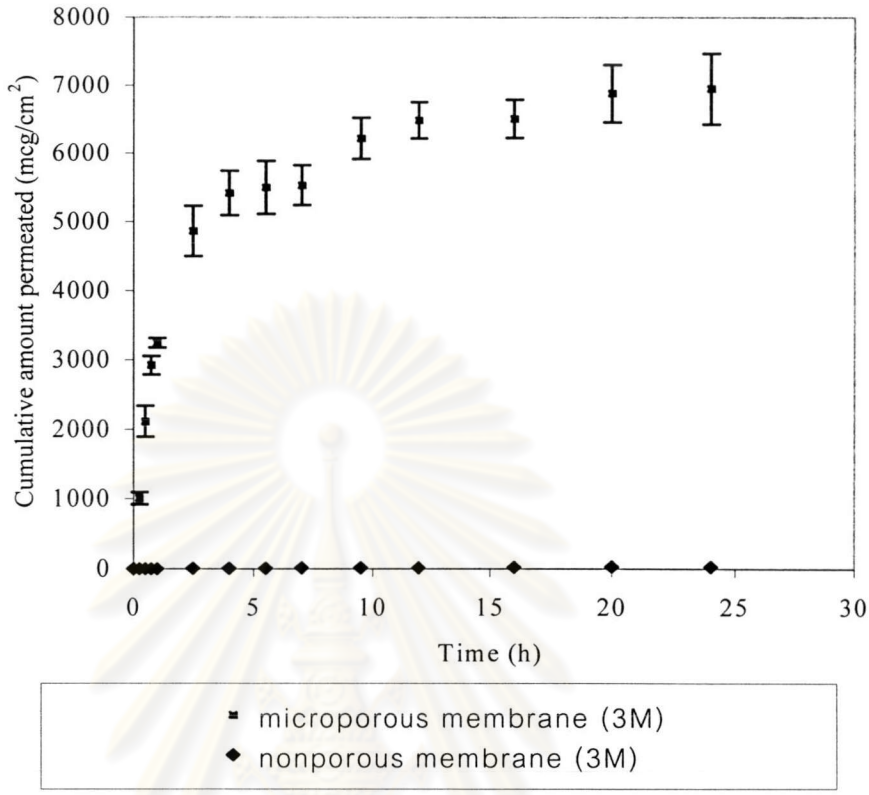

Figure 23 The release profiles of AZT from F14 across microporous membrane and nonporous membrane at 37± 1^0C (n=3, error bar = SE).

Table 23 Effect of controlling membrane on the release of AZT

Type of membrane	Lag time (SE) (h) (n=3)	Flux (SE) (mcg/cm^2/h) (n=3)	Permeability (Kp) x10^3 (SE) (cm/h) (n=3)
Microporous membrane	no	at 0-0.75 h 3951.27 (168.66) at 9.5-24 h 68.47 (10.76)	at 0-0.75 h 92.21 (3.94) at 9.5-24 1.57 (0.28)
Nonporous membrane	no	at 0-24 h 1.49 (0.04)	at 0-24 h 0.04 (0.003)

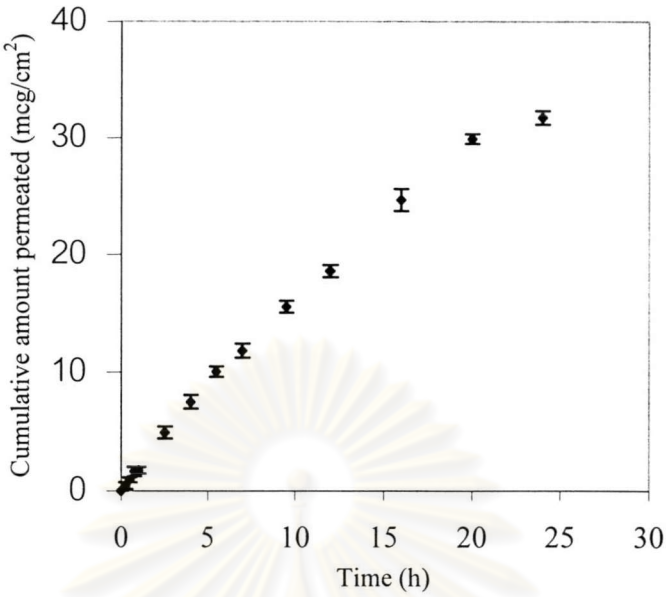

Figure 24 The release profile of AZT from F14 across 9% ethyl vinyl acetate nonporous membrane

3.2 Effect of controlling membrane on drug permeation study

The microporous membrane was selected from 3.1. Therefore, polyethylene membrane, PE, and polycarbonate membrane were investigated in this study.

The permeation profiles of AZT from F14 across newborn pig skin and permeate through two difference microporous membranes adhered on newborn pig skin are shown in Figure 25. These profiles had different lag time and slope. The lag times were not more than 7 h. AT 24 h, the cumulative amount of AZT permeated through PE was about 2300 mcg/cm^2, while about 1800 mcg/cm^2 was permeated through PC.

The lag time, flux, and permeability coefficient were calculated and summarized in Table 24. The lag time of AZT permeated through PE and PC were shorter than that permeated through skin alone. While, lag time from PE and PC were similar ($p>0.05$). This indicated that the microporous membrane caused increase in occlusion effect on the skin. Barry *et al.* (2001) suggested that occlusion patch, in most transdermal patches, prevents water loss so skin was full hydration.

AZT flux through PE and PC were reduced about two times of AZT permeated through skin alone. Although AZT concentrations in donor were the same, but AZT fluxes were decreased due to permeability coefficient decreased. However, fluxes from PE and PC were similar ($p>0.05$). In spite of the fact that PE and PC were difference in its micropore which were 0.2 mcm and 0.4 mcm, respectively. Due to these membranes micropore property so permeation parameters of them were not difference, moreover, formulation for drug release was also the same.

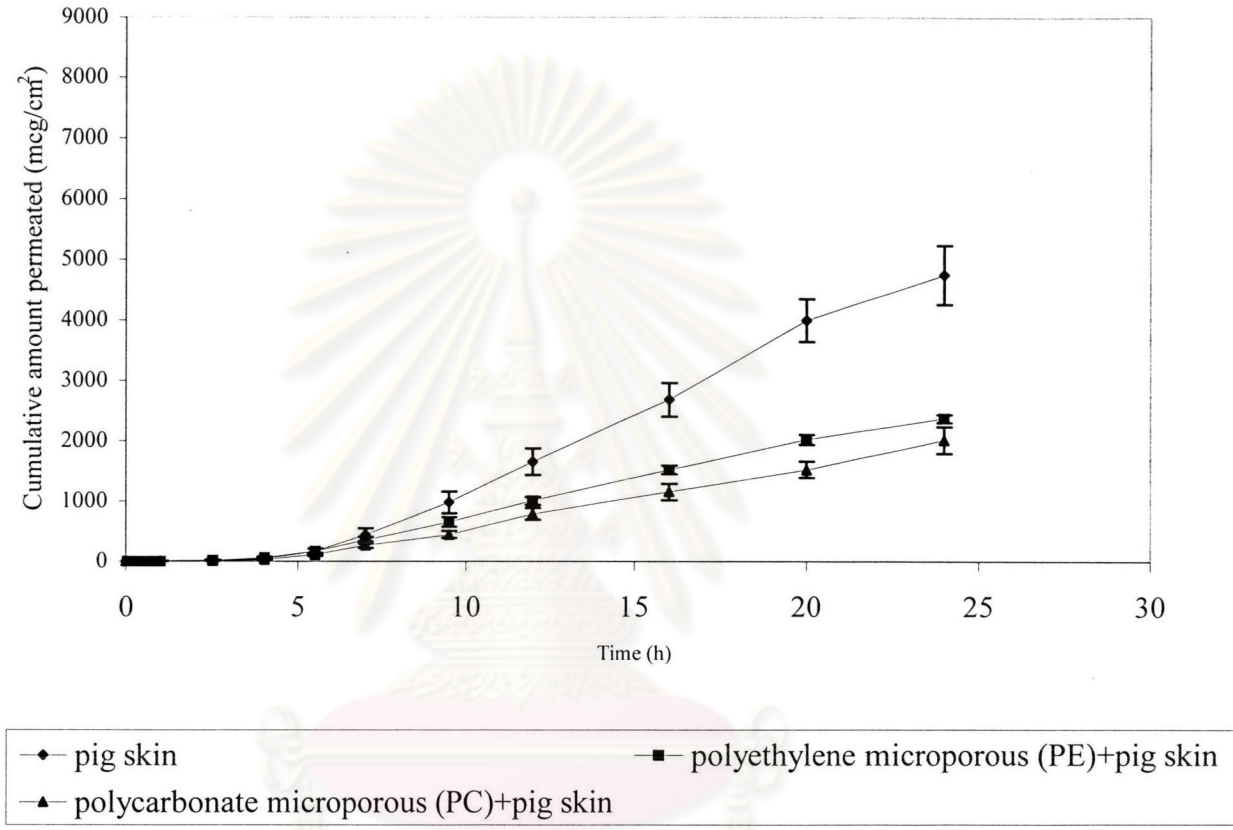

Figure 25 Permeation profiles of AZT from F14, at 37±1°C (n=5, error bar = SE).

Table 24 Permeation parameters of AZT from F14 and F23 across microporous membranes adhered on newborn pig skin.

Type of membrane	F14			F23		
	Lag time (SE) (h) (n=5)	Flux[a] (SE) (mcg/cm^2/)h (n=5))	Permeability (K_p) x10^3 (SE) (cm/h (n=5)	Lag time (SE) (h) (n=5)	Flux[a] (SE) (mcg/cm^2/)h (n=5))	Permeability (K_p) x10^3 (SE) (cm/h) (n=5)
Pig skin	6.25 (0.45)	284.92 (18.34)	6.74 (0.43)	7.49 (0.59)	460.34 (18.72)	8.16 (0.33)
PE microporous membrane	3.89 (0.56)	121.99 (3.28)	2.85 (0.08)	5.71 90.29)	215.31 (5.20)	3.22 (0.56)
PC microporous membrane	4.63 (0.28)	103.25 (8.63)	2.42 (0.20)	-	-	-
T – test between PE vs PC	NS (p>0.05)	NS (p>0.05)	NS (p>0.05)	-	-	-

[a] Assume steady state flux

The K_p values from PE and PC were less than two times of AZT permeated without membrane. However, the K_p values from PE and PC were similar ($p>0.05$). The thickness for AZT permeated through microporous membrane (10 mcm) adhered on skin was more than skin alone (about 200 mcm). Therefore, the K_p values were decreased due to the thickness for AZT diffusion increased. Moreover, the effects of binary vehicle and enhancer on skin were retarded by membrane. This because of the stratum corneum was modified either by vehicle or enhancer to less than AZT permeation through the skin without membrane. In general, the rate of transdermal permeation of a drug at steady state, $(R_p)_{ss}$, is mathematically related to the actual rate of drug delivery from a transdermal drug delivery system (TDDS), $(R_d)_a$, to the skin surface and the maximum achievable rate of skin absorption, $(R_a)_m$, by the following relationship (Chien, 1987):

$$1/((R_p)_{ss} = 1/(R_d)_a + 1/(R_a)_m \quad \text{.....(16)}$$

According to this equation, the rate of transdermal permeation of AZT at steady state was nearly the rate-limiting step. These results indicated that permeation rate of AZT across newborn pig skin was the rate-limiting step. Then the rate of AZT permeated through microporous membrane adhered on skin should be nearly the rate of AZT across skin alone. But they were reduced by a half when AZT permeated through skin alone. This indicated that the microporous membrane retarded AZT permeation, which in general permeation of AZT was enhanced by the effects of binary vehicle and enhancer on the skin. Therefore, AZT flux from F14 did not achieve target flux.

F23 had been another candidate for this study. The permeation profiles of AZT from F23 across pig skin and, PE microporous membrane adhered on skin are shown in Figure 26. These profiles have different lag time and slope. These lag times of about 5-7 h were observed. The cumulative amount AZT permeation through PE not more than 4000 mcg/cm^2, it less two times than AZT permeation through skin without membrane at 24 h.

The lag time, flux, and permeability coefficient were calculated and summarized in Table 24. The lag time of AZT permeation through PE adhered on skin was shorter than AZT permeation through skin without membrane. Because of an occlusion effect from membrane, which was described above. In addition, flux was reduced two times of AZT permeation when across the skin alone. However, this flux of 215.31 mcg/cm^2/h was still achieved to target flux. Although, permeability coefficient of AZT was reduced about twice when it was compared with AZT permeated through skin alone.

The cumulative amount of AZT 3885.65 mcg/cm^2 at 24 h (APPENDIX E), that it permeated through membrane and skin found to be 7033.03 mcg (surface area =1.81 cm^2). Therefore, AZT permeated from transdermal delivery system (TDS) was about 8.33 % of a formula (AZT concentration in donor = 56.25 mg/ml, volume 1.5 ml). Then this TDS system might be sustained AZT permeation for more than 24 h.

Ideally, a TDS should be so designed to have a transdermal permeation rate by using the rate of drug delivery from the TDS, not using the skin permeation rate. In such as a case, the transdermal bioavailability of a drug becomes less dependent upon the intra-and/or interpatient variabilities in skin permeability (Chien, 1987).

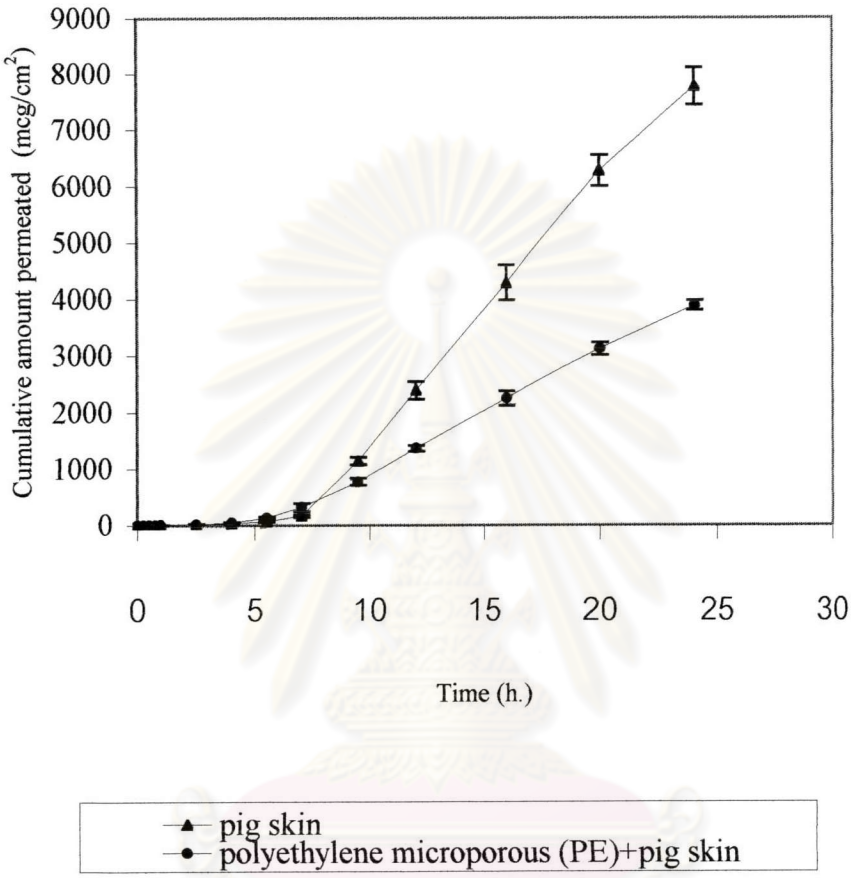

Figure 26 Permeation profiles of AZT from F23 at 37±1°C (n=5, error bar = SE).

However, AZT was poorly permeated through skin and a high therapeutic dose was required. The therapeutic dose of AZT for adult was 200 mg/ every 4 h. Then, the enhancing permeation through skin was difficult to achieved the therapeutic effect. But 10% NMP in ethanol/IPM (30/70) could improve AZT permeation to achieve the target flux (208 mcg/cm^2/h). Therefore, the feasibility of AZT development for TDS may be possible if it was designed to an appropriate TDS. The membrane-controlled system was interesting for AZT transdermal delivery system design when it was compared with other systems. However, nonporous membrane could not be possible because of it retarded almost all of the release of AZT from system. Although, the microporous membrane was not the rate-limiting step for TDS, however it might be possible approach for the future dosage form.